

Transport and Magnetic properties of laser ablated $\text{La}_{0.7}\text{Ce}_{0.3}\text{MnO}_3$ films on LaAlO_3 : Effect of oxygen pressure, sample thickness and co-doping with Ca

P. Raychaudhuri†, S. Mukherjee, A. K. Nigam, J. John, U. D. Vaisnav, R. Pinto
*Department of Condensed Matter and Materials Science, Tata Institute of Fundamental
Research, Homi Bhabha Rd., Colaba, Mumbai-400005, India.*

And

P. Mandal
Saha Institute of Nuclear Physics, Block-AF, Sector I, Salt Lake, Calcutta-700064.

Abstract: $\text{La}_{0.7}\text{Ce}_{0.3}\text{MnO}_3$ is a relatively new addition in the family of colossal magnetoresistive manganites where the cerium ion is believed to be in the Ce^{4+} state. In this paper we report an extensive study the magnetotransport properties of laser ablated $\text{La}_{0.7}\text{Ce}_{0.3}\text{MnO}_3$ films on LaAlO_3 with variation in ambient oxygen pressure during growth and film thickness. We observe that the transport and magnetic properties of the film depend on the interplay between oxygen pressure, surface morphology, film thickness and epitaxial strain. The films were characterized by x-ray diffraction on a 4-circle x-ray goniometer. We observe an increase in the metal-insulator transition temperature with decreasing oxygen pressure. This is in direct contrast with the oxygen pressure dependence of $\text{La}_{0.7}\text{Ca}_{0.3}\text{MnO}_3$ films suggesting the electron doped nature of the $\text{La}_{0.7}\text{Ce}_{0.3}\text{MnO}_3$ system. With decreasing film thickness we observe an increase in the metal-insulator transition temperature. This is associated with a compression of the unit cell in the a-b plane due to epitaxial strain. When the system is co-doped with 50% Ca at the Ce site the system ($\text{La}_{0.7}\text{Ca}_{0.15}\text{Ce}_{0.15}\text{MnO}_3$) is driven into a insulating state suggesting that the electrons generated by Ce^{4+} is compensated by the holes generated by Ca^{2+} valence thus making the average valence at the rare-earth site $3+$ as in the parent material LaMnO_3 .

† e-mail: pratap@tifr.res.in

I. Introduction

Hole doped rare-earth manganites of the form RMnO_3 ($\text{R} = \text{rare-earth}$) have attracted a lot of attention in recent times due their interesting magnetotransport properties arising from spin charge coupling. The parent material is a charge transfer insulator¹ where the Mn^{3+} moments form a layered antiferromagnetic structure. The electronic configuration of Mn^{3+} is $t_{2g}^3 e_g^1$ where the three t_{2g} electrons are tightly bound with a net spin of $3/2$. Hole doping is achieved in these compounds by substituting a bivalent cation like Ca, Sr, Pb at the rare-earth site. Around 30% doping compounds like $\text{La}_{0.7}\text{Ca}_{0.3}\text{MnO}_3$ show ferromagnetism associated with a metal-insulator transition and large negative magnetoresistance close to the ferromagnetic transition temperature (T_c). These exotic properties of these material arise due to the strong on site Hund's rule coupling between the localized t_{2g}^3 electrons and the electrons in the e_g band. This gives rise to a coupling between neighboring $\text{Mn}^{3+}/\text{Mn}^{4+}$ pairs are coupled via Zener double exchange² mechanism. According to this mechanism the hopping probability of an electron between two neighboring $\text{Mn}^{3+}/\text{Mn}^{4+}$ pairs is proportional to $\cos(\theta/2)$ ³. $\text{La}_{0.7}\text{Ce}_{0.3}\text{MnO}_3$ is unique in this family of compounds since the trivalent La is replaced by Ce instead of a bivalent cation. This compound has orthogonal structure with $a \approx b \approx \sqrt{2}c$. This compound shows metal-insulator transition^{4,5} and ferromagnetism associated with large negative magnetoresistance similar to $\text{La}_{0.7}\text{Ca}_{0.3}\text{MnO}_3$. To explain the observed behavior P. Mandal and S. Das⁶ have argued that Ce could exist in in Ce^{4+} state like in CeO_2 thus doping electrons instead of holes in the parent material. Thus according to their picture the double exchange in this compound operates between $\text{Mn}^{2+}/\text{Mn}^{3+}$ neighboring pairs giving

rise to metal insulator transition and ferromagnetism. From the theoretical point of view the double exchange mechanism is symmetric with respect to electron or hole doping in the parent compound. Incidentally, some of the present authors had reported metal-insulator transition and ferromagnetism in the electron doped layered manganite $\text{La}_{1.8}\text{Y}_{0.5}\text{Ca}_{0.7}\text{Mn}_2\text{O}_7$ ^{7,8}.

In this paper we report a detail study of $\text{La}_{0.7}\text{Ce}_{0.3}\text{MnO}_3$ films prepared by pulsed laser ablation on LaAlO_3 . In some cases we also prepared $\text{La}_{0.7}\text{Ca}_{0.3}\text{MnO}_3$ films for comparison with these films. We compare the effect of ambient oxygen pressure during growth on $\text{La}_{0.7}\text{Ce}_{0.3}\text{MnO}_3$ and $\text{La}_{0.7}\text{Ca}_{0.3}\text{MnO}_3$ films. To address the question of the valence state of Ce we prepared films of nominal composition $\text{La}_{0.7}(\text{Ce}_{0.15}\text{Ca}_{0.15})\text{MnO}_3$. This compound goes into an insulating state when the film is grown at 100mTorr oxygen pressure suggesting that the electrons generated by Ce^{4+} compensate the holes generated by Ca^{2+} . Finally, we study the effect epitaxial strain on the metal-insulator transition temperature (T_p) by varying the film thickness.

II. Experiment

Films of $\text{La}_{0.7}\text{Ce}_{0.3}\text{MnO}_3$, $\text{La}_{0.7}\text{Ca}_{0.3}\text{MnO}_3$ and $\text{La}_{0.7}\text{Ce}_{0.15}\text{Ca}_{0.15}\text{MnO}_3$ were prepared by pulsed laser deposition using a KrF excimer laser in oxygen atmosphere. The substrate temperature was kept between 750-770⁰C for all the films. The laser energy density was kept at roughly 160mJ/mm² per shot with a repetition rate of 10Hz. Films were grown at 3 oxygen pressures: 100mTorr, 200mTorr, 400mTorr. Films used for thickness dependence study were all grown at 400mTorr. After deposition the laser ablation chamber was vented with high purity oxygen and the substrate cooled down to room temperature. The lattice parameters of the films by x-ray diffraction on a high resolution 4-circle x-ray goniometer.

Film thickness was measured using stylus method on a Dektak profilometer. Resistance and magnetoresistance were measured by conventional 4-probe technique. Magnetization was measured on a Quantum Design superconducting quantum interference device (SQUID) magnetometer. Surface morphology was checked using a Digital Instrument atomic force microscope.

III. Results and discussion

A. Effect of ambient oxygen pressure during growth:

To study the effect of oxygen pressure on metal insulator transition (T_c) and the ferromagnetic transition (T_p) films of $\text{La}_{0.7}\text{Ce}_{0.3}\text{MnO}_3$ were grown at 3 different oxygen pressures: 100mTorr, 200mTorr and 400mTorr. Other parameters like deposition time, laser energy, and substrate temperature were kept constant for all the films. For comparison the $\text{La}_{0.7}\text{Ca}_{0.3}\text{MnO}_3$ films were also grown under the same conditions. All the films were seen to have $c \perp$ (film plane) from the x-ray $\theta-2\theta$ scan. Figure 1 shows a representative x-ray diffraction $\theta-2\theta$ scans of the $\text{La}_{0.7}\text{Ce}_{0.3}\text{MnO}_3$ film grown at 400mTorr showing the (00n) peaks. Figures 2a-f show the atomic force microscope (AFM) image of the three $\text{La}_{0.7}\text{Ce}_{0.3}\text{MnO}_3$ and $\text{La}_{0.7}\text{Ca}_{0.3}\text{MnO}_3$ film surfaces. There is a degradation of the surface morphology and grain size for the $\text{La}_{0.7}\text{Ce}_{0.3}\text{MnO}_3$ film grown at low oxygen pressure (100mTorr) (figure 2c). This degradation in the surface morphology at low oxygen pressure is also observed in $\text{La}_{0.7}\text{Ca}_{0.3}\text{MnO}_3$ films grown at 100mTorr (figure 2f). Figures 3a-c show the resistance versus temperature (R-T) from for the three films. The interesting fact is that the metal-insulator transition temperature (T_p) and the ferromagnetic transition temperature (T_c) increases from 246K for the film grown at 400mTorr to 272K for the film grown at 100mTorr. However, the effect of ambient

oxygen pressure on T_p in $\text{La}_{0.7}\text{Ce}_{0.3}\text{MnO}_3$ is in direct contrast to the effect of ambient oxygen pressure on T_p in $\text{La}_{0.7}\text{Ca}_{0.3}\text{MnO}_3$. Figures 3d-f show the R-T curves for $\text{La}_{0.7}\text{Ca}_{0.3}\text{MnO}_3$ films grown at the same pressures. In the case of $\text{La}_{0.7}\text{Ca}_{0.3}\text{MnO}_3$ the metal-insulator transition broadens drastically with decreasing oxygen pressure with a small decreasing trend in T_p . Before elaborating further on these results we shall discuss the effect of co-doping Ce and Ca in $\text{La}_{0.7}\text{Ce}_{0.15}\text{Ca}_{0.15}\text{MnO}_3$. However, we would like to point out that this property might be useful from the technological point of view since this allows $\text{La}_{0.7}\text{Ce}_{0.3}\text{MnO}_3$ films to be synthesized on a wider range of oxygen pressures without compromising on the metal-insulator transition width.

In spite of the initial picture proposed in ref.6 electron doping in $\text{La}_{0.7}\text{Ce}_{0.3}\text{MnO}_3$ via Ce^{4+} valence state has been a questionable issue since the data of thermo-electric power (TEP) in this material (bulk) is similar to that of hole doped manganites. However, the analysis TEP data in these materials could be very complex, in particular where the TEP changes sign as a function of temperature⁶. To resolve this problem we prepared films of the nominal composition $\text{La}_{0.7}\text{Ce}_{0.15}\text{Ca}_{0.15}\text{MnO}_3$. If Ce is in the 4+ state one would expect the holes generated by Ca^{2+} be compensated by the electrons generated by Ce^{4+} thus driving the system into an insulating state like in the parent compound LaMnO_3 . The difficulty in this is that the undoped compound (like LaMnO_3) has a tendency to get overoxygenated, generating cation vacancies^{9,10,11}. It has been shown that the overoxygenated compound can show a metal-insulator transition just like the doped material¹². However, if the compound $\text{La}_{0.7}\text{Ce}_{0.15}\text{Ca}_{0.15}\text{MnO}_3$ is compensated for electrons and holes the effect of varying ambient oxygen pressure during growth should be much more drastic than in $\text{La}_{0.7}\text{Ca}_{0.3}\text{MnO}_3$ or $\text{La}_{0.7}\text{Ce}_{0.3}\text{MnO}_3$ films since one should be able to

suppress the carriers by decreasing the oxygen pressure. In figure 4a-b we show the R-T curve for $\text{La}_{0.7}\text{Ce}_{0.15}\text{Ca}_{0.15}\text{MnO}_3$ films grown at 400mTorr and 100mTorr oxygen pressure. The film grown at 400mTorr shows a metal-insulator transition around 230K. However, the film grown at 100mTorr becomes an insulator with resistance 4 orders of magnitude larger than the films grown at 400mTorr at 55K. Comparing this result with the effect of varying oxygen pressure in the same range in $\text{La}_{0.7}\text{Ca}_{0.3}\text{MnO}_3$ and $\text{La}_{0.7}\text{Ce}_{0.3}\text{MnO}_3$ (figure 3) we see that the low temperature metallic phase in these two compounds is never fully suppressed. The drastic increase in the resistance and the suppression of metallicity in the $\text{La}_{0.7}\text{Ce}_{0.15}\text{Ca}_{0.15}\text{MnO}_3$ film grown at 100mTorr thus indicates that electrons and holes are compensated in this compound.

Having thus established that Ce is in 4+ state one can now look more carefully at the data on $\text{La}_{0.7}\text{Ce}_{0.3}\text{MnO}_3$ and $\text{La}_{0.7}\text{Ca}_{0.3}\text{MnO}_3$ in figure 3. Firstly the increase in T_p with decreasing oxygen pressure in $\text{La}_{0.7}\text{Ce}_{0.3}\text{MnO}_3$ could be understood as follows. The parent compound LaMnO_3 the Mn ion has a filled t_{2g} orbital with three electrons and one electron at the e_g orbital. The average occupancy at the e_g orbital (n) is therefore 1. The twofold degeneracy of the e_g orbital is lifted in due to the Jahn-Teller distortion in LaMnO_3 making the material an insulator. In $\text{La}_{0.7}\text{Ca}_{0.3}\text{MnO}_3$ the parent compound is doped with holes and the average occupancy $0 < n < 1$. On the other hand in $\text{La}_{0.7}\text{Ce}_{0.3}\text{MnO}_3$ the parent compound is doped with electrons and $1 < n < 2$. Since the oxygen content of the film depends on the ambient oxygen pressure during growth we assume the $\text{La}_{0.7}\text{Ce}_{0.3}\text{MnO}_3$ film to have the composition $\text{La}_{0.7}\text{Ce}_{0.3}\text{MnO}_{3-\delta}$. (We wish to point out that at this point we do not attach too much significance to the negative sign of δ since it is not known whether this material gets overoxygenated or under oxygenated. δ is used at this point to relatively compare

films with different oxygen stoichiometry). For this composition the average valence of Mn is $2.7-2\delta$. This means that when δ is increased the average manganese valence reduces towards 2. This in turn increases the electron doping at the e_g orbital. This is in contrast to the situation in the hole doped $\text{La}_{0.7}\text{Ca}_{0.3}\text{MnO}_{3-\delta}$. In this case the average Mn valence is $3.3-2\delta$. Here increasing δ means that the Mn valence will reduce towards 3 thus decreasing hole doping. Thus in terms of doping the reducing oxygen pressure has opposite effect in the two compounds. This is schematically shown in figure 5. (The e_g band in these compounds are spin split due to the large on-site Hund's rule coupling.) Since T_p and T_c are known to be sensitive function of doping in these materials this could give rise to increase in T_p in one case and decrease in the other. The other difference between $\text{La}_{0.7}\text{Ca}_{0.3}\text{MnO}_3$ and $\text{La}_{0.7}\text{Ce}_{0.3}\text{MnO}_3$ films is that the width of the metal-insulator transition is much less affected by the decrease in the oxygen pressure in $\text{La}_{0.7}\text{Ce}_{0.3}\text{MnO}_3$. For the $\text{La}_{0.7}\text{Ca}_{0.3}\text{MnO}_3$ film grown at 100mTorr the metal-insulator transition becomes extremely wide (figure 3f). On the other hand the width of the transition remains almost constant (with a slight decrease at lower oxygen pressures) with decrease in oxygen pressure for $\text{La}_{0.7}\text{Ce}_{0.3}\text{MnO}_3$ film (figure 3g). The large broadening in the metal-insulator transition in $\text{La}_{0.7}\text{Ca}_{0.3}\text{MnO}_3$ suggest that the $\text{La}_{0.7}\text{Ca}_{0.3}\text{MnO}_3$ films becomes inhomogeneously oxidized at lower oxygen pressures. We believe that the $\text{La}_{0.7}\text{Ce}_{0.3}\text{MnO}_3$ film is more homogeneous in terms of its oxygen stoichiometry due to the high oxygen affinity of cerium. This robustness of the metal-insulator transition might be advantageous from the application point of view where a sharp metal-insulator transition and a large temperature coefficient of resistivity is desirable, for example, in the case of bolometric application of perovskite manganite films^{13,14}.

B. The effect of epitaxial strain on the metal-insulator transition (T_p) and magnetoresistance:

In order to study the effect of epitaxial strain on the transport properties of this material we synthesized films in of varying thickness in the range 500-3200 Å. For the thinnest film the thickness was estimated from the deposition time. The substrate temperature was kept at 760⁰C and the ambient oxygen pressure was kept at 400mTorr during growth. These values were chosen since grain size and surface morphology was best for these parameters. Figure 6a-c show the surface morphology for films of various thicknesses. Thicker films have smaller grain size possibly due to strain relaxation. In figure 7a we show the R-T curves close to the metal insulator transition. There is a gradual increase in T_p with decreasing film thickness. However we see that there is not much change in the width of the metal-insulator transition in this thickness range. This is shown in figure 7b where R/R_{\max} is plotted as a function of T/T_p . Figure 7c shows the magnetoresistance ($MR \sim \Delta\rho/\rho_0 \sim (\rho(H) - \rho(0))/\rho(0)$) at 300 K for the four samples. There is a gradual increase in the magnetoresistance with decreasing film thickness.

In order to understand this phenomenon we measured the lattice constant of the 4 films using X-ray diffraction on a 4-circle high resolution X-ray goniometer. The lattice constants along with the cell volume a T_p for films of various thickness are summarized in Table I. There is a gradual compression in the in-plane (a-b) lattice constants with decreasing thickness associated with a expansion in the c-axis lattice parameter. This is understandable since the pseudo-cubic lattice parameter of LaAlO_3 is smaller than the pseudo-cubic lattice parameters of $\text{La}_{0.7}\text{Ce}_{0.3}\text{MnO}_3$. To understand the increase in T_p with

decrease in thickness we note that T_p in the bulk compound increases with applied pressure¹⁵. It has been shown that T_p (and T_c) in doped manganites is governed by the bandwidth (W) of the e_g band and is given by the semi empirical formula¹⁶

$$W \propto \frac{\cos\omega}{d_{\text{Mn-O}}^{3.5}},$$

where ω is the “tilt” angle in the plane of the Mn-O-Mn bond (given by $\omega = \frac{1}{2}(\pi - \langle \text{Mn - O - Mn} \rangle)$), $d_{\text{Mn-O}}$ is the Mn-O bond length. The applied isotropic pressure in bulk samples reduces $d_{\text{Mn-O}}$ but keeps ω almost constant thus increasing W and T_c . On the other hand when a chemical pressure is applied by modifying the size of the cation at the rare-earth site $\cos\omega$ decreases more rapidly than $d_{\text{Mn-O}}$ thus reducing W and T_c . We believe that the effect of compressive epitaxial stress in films is similar to the applied pressure in the bulk sample. However the situation is more complicated here due to anisotropic in-plane and out of plane strain in the film which give rise to different values of $d_{\text{Mn-O}}$ and ω in different directions. R. A. Rao et al¹⁷ have reported the effect of epitaxial strain in $\text{La}_{0.8}\text{Ca}_{0.2}\text{MnO}_3$ films of varying thickness. Their study revealed that T_p decreases with compressive in-plane epitaxial strain. The puzzling fact is that in bulk $\text{La}_{0.7}\text{Ca}_{0.3}\text{MnO}_3$ also T_p increases with applied pressure¹⁶. M. G. Blamire et al¹⁸ have reported similar results on laser ablated $\text{La}_{0.7}\text{Ca}_{0.3}\text{MnO}_3$ films on LaAlO_3 and SrTiO_3 . A close inspection of their R-T data for various film thicknesses reveal that the metal-insulator transition becomes extremely broad in addition to the decrease in T_p with decreasing film thickness. One reason for this behavior could be that very thin films of $\text{La}_{0.7}\text{Ca}_{0.3}\text{MnO}_3$ tend to lose oxygen thereby reducing its T_p ¹⁷.

Figure 7a-d show the R-T curves close to the metal-insulator transition for the films with varying thickness at different fields up to 1.5T. All the films have a large MR > 60% close to the metal-insulator transition at 1.5T (Figure 7e). One point to note here is that above 250K thinner films have larger MR. This could be useful from the application point of view since a large MR at temperatures close to room temperature is required for the device application of these films.

IV. Conclusion

In summary, we have reported in this paper the magnetic and transport properties of laser ablated $\text{La}_{0.7}\text{Ce}_{0.3}\text{MnO}_3$ films on LaAlO_3 substrates. By co-doping with Ca in $\text{La}_{0.7}\text{Ca}_{0.15}\text{Ce}_{0.15}\text{MnO}_3$ we have established that in this system the parent compound (LaMnO_3) is doped with electrons in contrast to the hole doped compounds like $\text{La}_{0.7}\text{Ca}_{0.3}\text{MnO}_3$ where holes are doped by substitution of bivalent Ca^{2+} at the rare-earth site. We have compared the effect of ambient oxygen pressure during growth in $\text{La}_{0.7}\text{Ca}_{0.3}\text{MnO}_3$ and $\text{La}_{0.7}\text{Ce}_{0.3}\text{MnO}_3$. We find that the latter is much more stable with respect to variation in oxygen pressure. Thickness dependence studies reveal that the metal-insulator transition temperature increases with decreasing thickness. This can be attributed to the compressive in-plane epitaxial strain in film. In conclusion, the properties of $\text{La}_{0.7}\text{Ce}_{0.3}\text{MnO}_3$ provide a scheme to tune the metal-insulator transition temperature over a moderate range in this colossal magnetoresistive manganite by varying oxygen pressure during growth and sample thickness without compromising on the sharpness of the metal-insulator transition.

Acknowledgement

We would like to thank G.S.Nathan for being involved in a part of this work. We also thank R.S.Sannabhadti and Arun Patade for technical support.

References:

1. J. Zaanen, G. A. Sawatzky and J. W. Allen, **Phys. Rev. Lett.** **55**, 418 (1985)
2. C. Zener, **Phys. Rev.** **82**, 403 (1951)
3. P. W. Anderson and H. Hasegawa, **Phys. Rev.** **100**, 675 (1955)
4. S. Das and P. Mandal, **Indian J. Phys.** **71**, 231(1997)

5. S. Das and P. Mandal, **Z. Phys. B** **104**, 7 (1997)
6. P. Mandal and S. Das, **Phys. Rev.** **B56**, 15073 (1997)
7. P. Raychaudhuri, C. Mitra, A. Paramekanti, R. Pinto, A. K. Nigam and S. K. Dhar, **J. Phys.: Condens. Matter** **10**, L191 (1998)
8. P. Raychaudhuri, A. K. Nigam, C. Mitra, S. K. Dhar, R. Pinto, **Physica B** **259**, 835 (1999)
9. J. H. Kuo, H. U. Anderson and D. M. Sparlin, **J. Solid State Chem.** **83**, 52 (1989)
10. M. Hervieu, R. Mahesh, N. Rangavittal, and C. N. R. Rao, **Eur. J. Solid State Inorg. Chem.** **32**, 79 (1995)
11. J. A. M. van Roosmalen and E. H. P. Cordfunke, **J. Solid State Chem.** **110**, 100 (1994)
12. J. Töpfer and J. B. Goodenough, **J. Solid State Chem.** **130**, 117 (1997)
13. A. Goyal, M. Rajeswari, R. Shreekala, S. E. Lofland, S. M. Bhagat, T. Boettcher, C. Kwon, R. Ramesh, and T. Venkatesan, **Appl. Phys. Lett.** **71**, 2535 (1997)
14. M. Rajeswari, C. H. Chen, A. Goyal, C. Kwon, M. C. Robson, R. Ramesh, T. Venkatesan and S. Lakeou, **Appl. Phys. Lett.** **68**, 3555, (1996)
15. S. Das, P. Mandal, R. Rawat, I. Das, (unpublished)
16. P. G. Radaelli, G. Iannone, M. Marezio, H. Y. Hwang, S-W. Cheong, J. D. Jorgensen and D. N. Argyriou, **Phys. Rev B****56**, 8265 (1997)
17. R. A. Rao, D. Lavric, T. K. Nath, C. B. Eom, L. Wu, and F. Tsui, **Appl. Phys. Lett.** **73**, 3294 (1998)
18. M. G. Blamire, B.-S. Teo, J. H. Durrell, N. D. Mathur, Z. H. Barber, J. L. McManus Driscoll, L. F. Cohen, and J. E. Evetts, **J. Magn. Magn. Mater.** **191**, 359 (1999)

Figure Captions:

Figure 1: X-ray $\theta-2\theta$ scan of the $\text{La}_{0.7}\text{Ce}_{0.3}\text{MnO}_3$ film grown at 400mTorr showing the (00n) peaks of the orthorhombic structure.

Figure 2: AFM photograph of the $\text{La}_{0.7}\text{Ce}_{0.3}\text{MnO}_3$ films grown at (a) 400mTorr, (b) 200mTorr, (c) 100mTorr. AFM photograph of the $\text{La}_{0.7}\text{Ca}_{0.3}\text{MnO}_3$ films grown at (d) 400mTorr, (e) 200mTorr, (f) 100mTorr.

Figure 3: Resistance versus temperature of $\text{La}_{0.7}\text{Ce}_{0.3}\text{MnO}_3$ grown at (a) 400 mTorr, (b) 200mTorr, (c) 100mTorr. Resistance versus temperature of $\text{La}_{0.7}\text{Ca}_{0.3}\text{MnO}_3$ grown at (d) 400 mTorr, (e) 200mTorr, (f) 100mTorr; (g) shows the R/R_{\max} versus T/T_p for the three $\text{La}_{0.7}\text{Ce}_{0.3}\text{MnO}_3$ films where R_{\max} is the resistance value at T_p .

Figure 4: Resistance versus temperature for $\text{La}_{0.7}\text{Ca}_{0.15}\text{Ce}_{0.15}\text{MnO}_3$ films grown at (a) 400 mTorr and (b) 100mTorr oxygen pressure.

Figure 5: Schematic band structure of $\text{La}_{0.7}\text{Ca}_{0.3}\text{MnO}_{3-\delta}$ and $\text{La}_{0.7}\text{Ce}_{0.3}\text{MnO}_{3-\delta}$. The Fermi energy E_F increases with in both cases with increase in δ . However this corresponds to decrease in hole doping in $\text{La}_{0.7}\text{Ca}_{0.3}\text{MnO}_{3-\delta}$ whereas in $\text{La}_{0.7}\text{Ce}_{0.3}\text{MnO}_{3-\delta}$ this increases the electron doping in the parent material.

Figure 6: Surface morphology of $\text{La}_{0.7}\text{Ce}_{0.3}\text{MnO}_3$ films of various thickness: (a) 500 Å (b) 1000 Å (c) 3200 Å.

Figure 7: (a) Resistance versus temperature around T_p for films of various thickness; (b) R/R_{\max} versus T/T_p for films of various thickness; (c) MR versus field at 300 K for films of various thickness.

Figure 8: (a)-(d) Resistance versus temperature at different fields for various film thickness. (e) MR at 1.5 T as a function of temperature for films of various thickness.

Table Caption

Table I: Evolution of lattice parameters, cell volume and T_p with thickness variation in $\text{La}_{0.7}\text{Ce}_{0.3}\text{MnO}_3$ films.

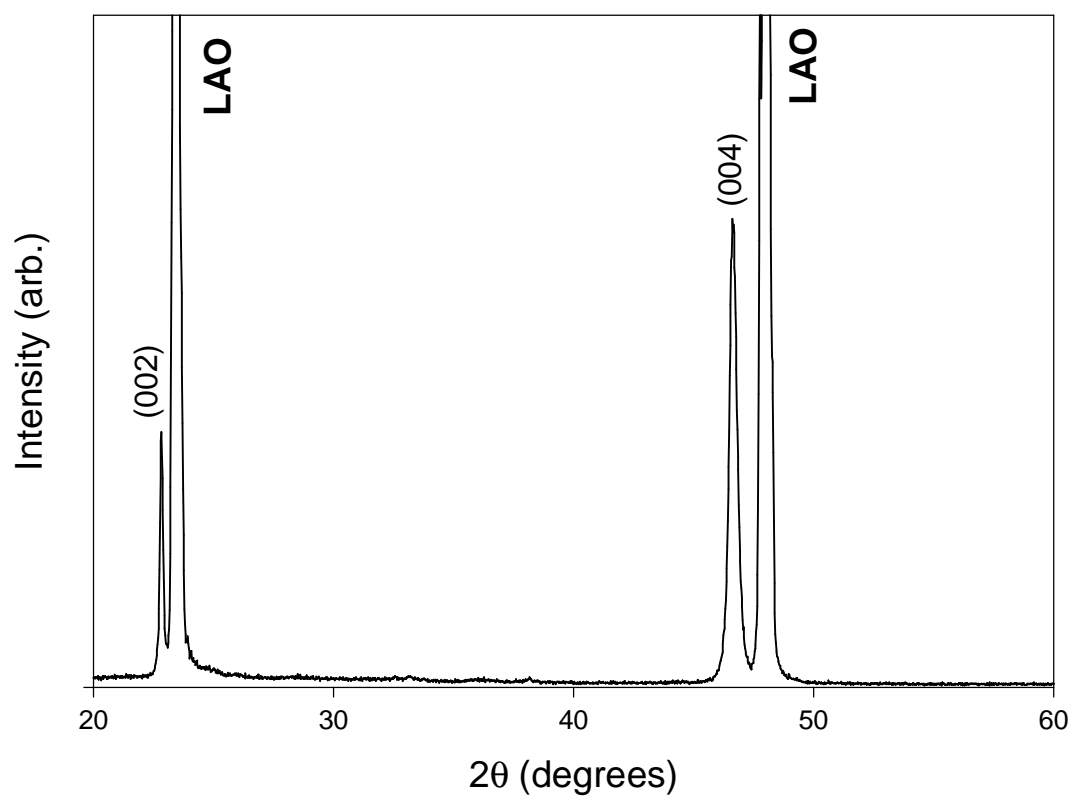


Figure 1 (P Raychaudhuri et.al.)

This figure "fig2r.jpg" is available in "jpg" format from:

<http://arxiv.org/ps/cond-mat/9905108v1>

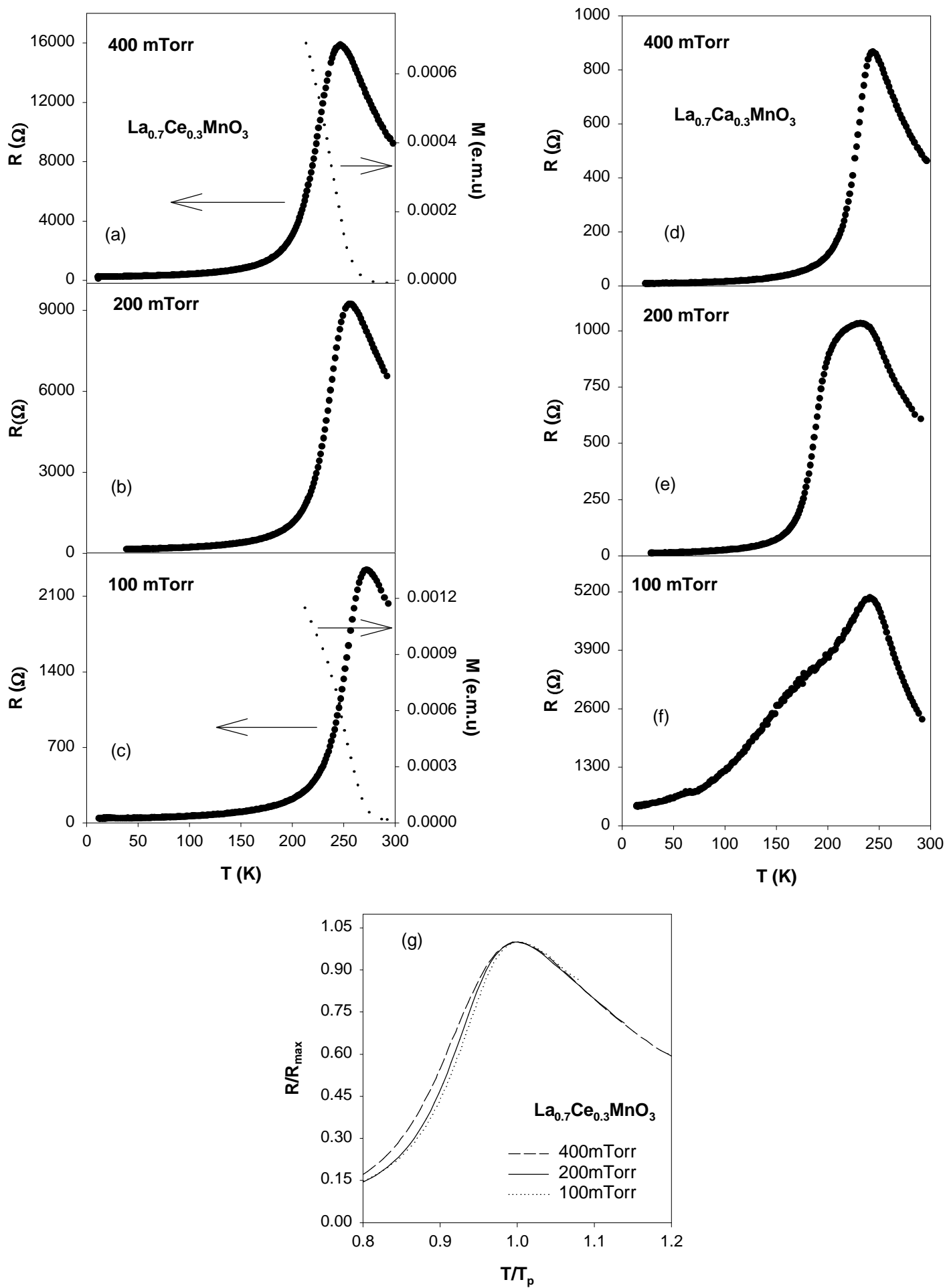


Figure 3 (P. Ravchaudhuri et al)

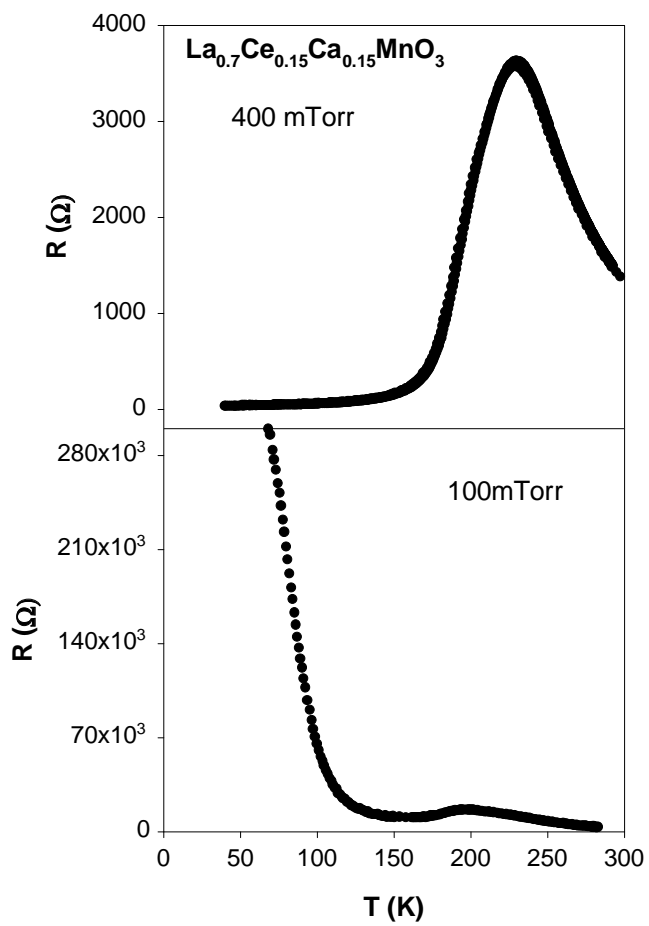


Figure 4 (P Raychaudhuri et al)

This figure "fig5.jpg" is available in "jpg" format from:

<http://arxiv.org/ps/cond-mat/9905108v1>

This figure "fig6.jpg" is available in "jpg" format from:

<http://arxiv.org/ps/cond-mat/9905108v1>

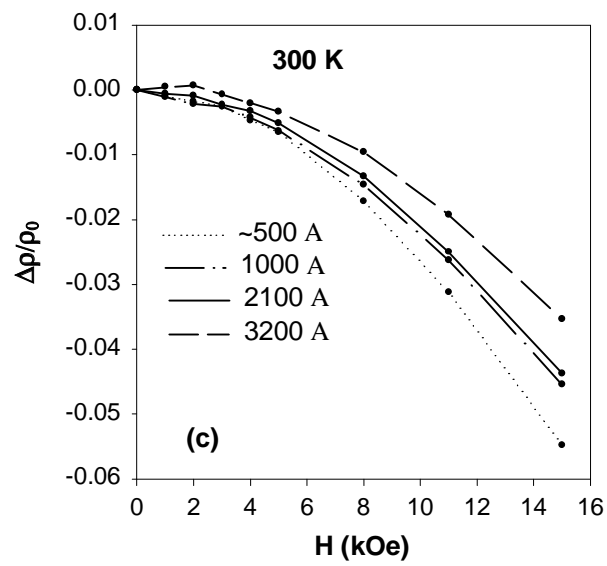
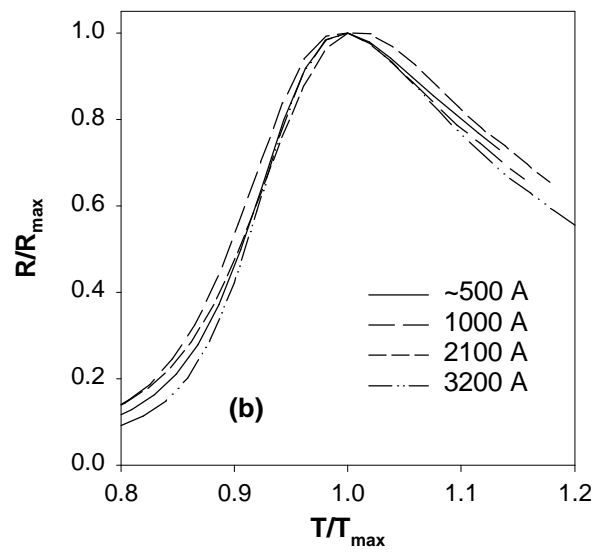
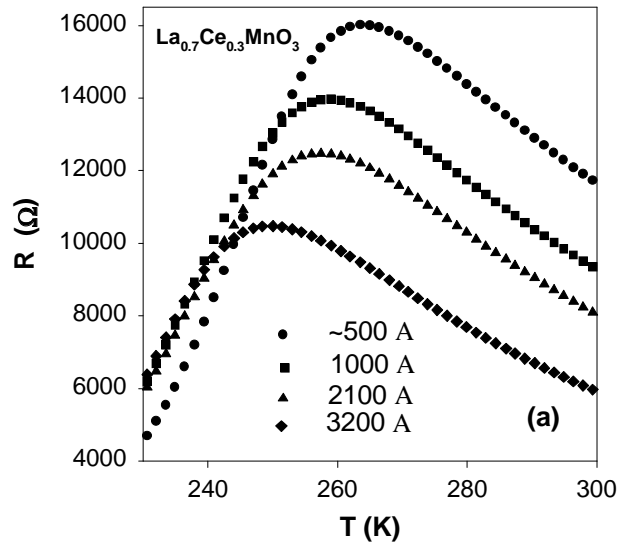


Figure 7 (P Raychaudhuri et al)

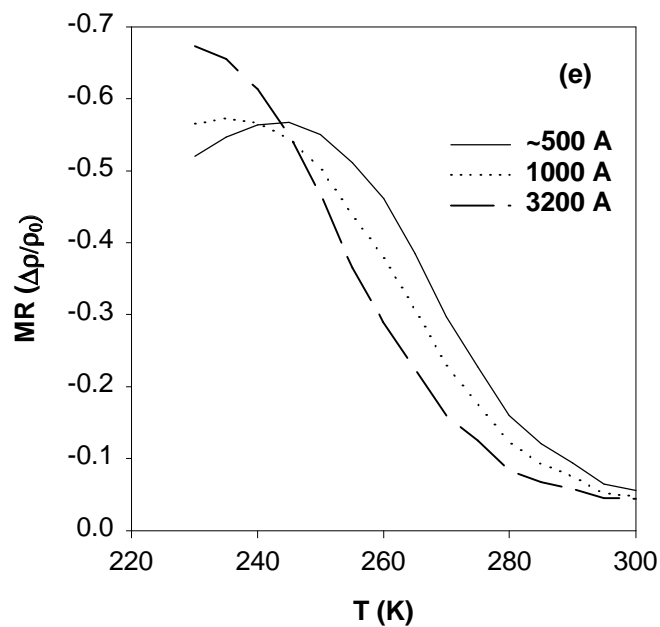
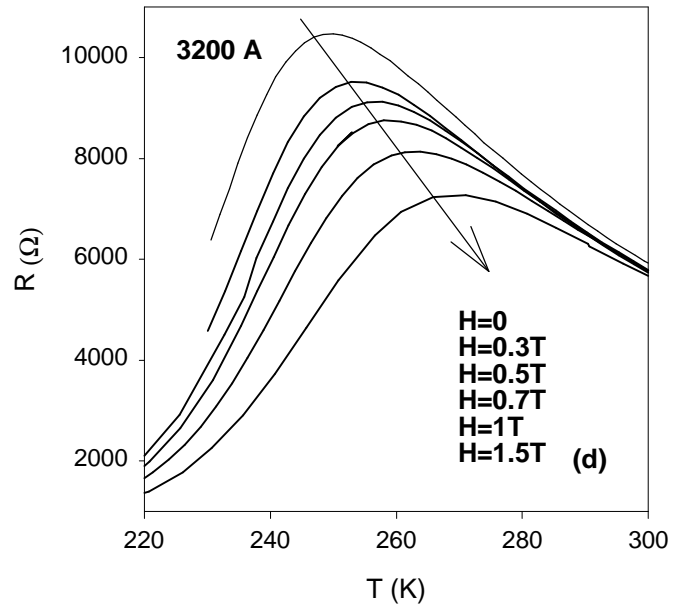
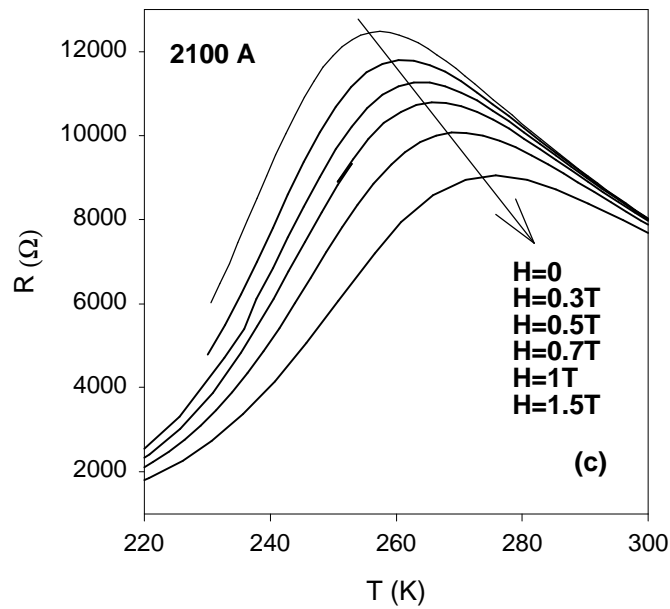
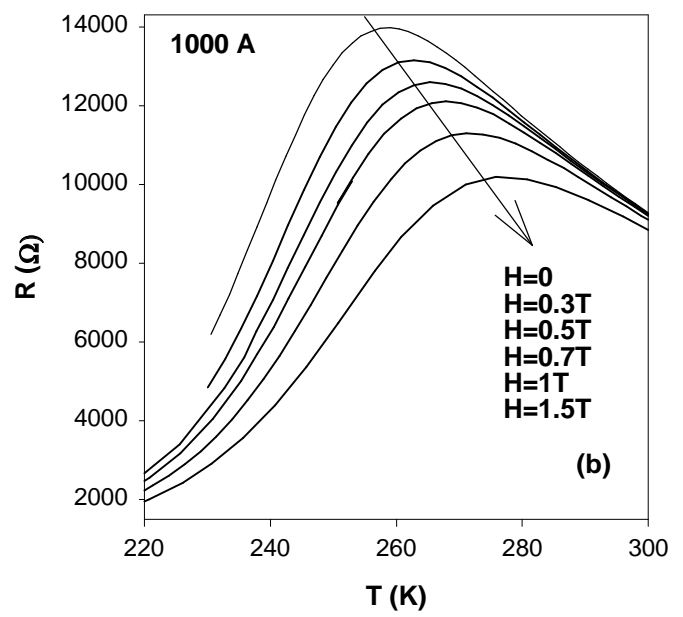
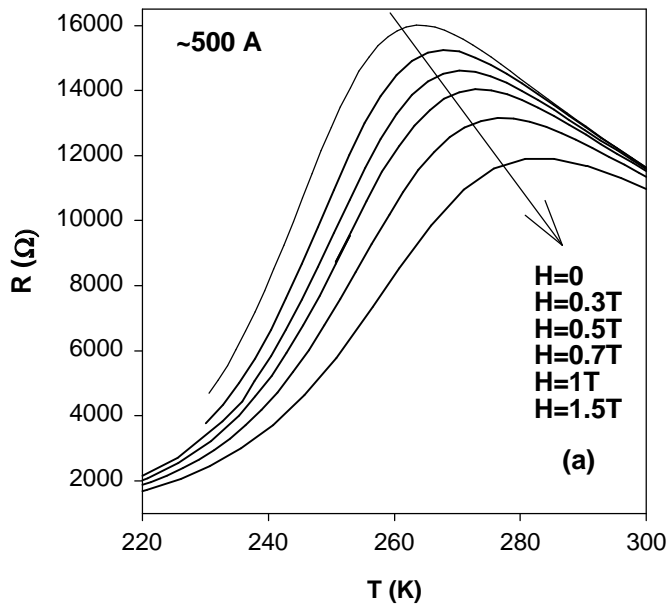


Figure 8 (P Raychaudhuri et al)

Table I

Thickness* (Å)	a (Å)	b (Å)	c (Å)	V (Å ³)	T _p (K)
500	5.518	5.459	7.852	236.52	263
1000±100	5.529	5.466	7.841	236.09	259
2100±100	5.548	5.464	7.836	237.54	257
3200±100	5.561	5.512	7.802	239.15	250

*All thickness values except the lowest one were measured on a Dektak profilometer. The lowest thickness was estimated from the time of deposition using the calibration from the thicker ones.